DEUTSCHES ELEKTRONEN-SYNCHROTRON DESY

DESY 82-065
September 1982

# SUMMARY OF THE SESSIONS ON LEPTON-HADRON PHYSICS

by

D. Haidt

NOTKESTRASSE 85 · 2 HAMBURG 52

DESY
Bibliothek
Notkestrasse 85
2 Hamburg 52
Germany

DESY 82-065
September 1982

# Summary of the sessions on Lepton-Hadron Physics

D. Haidt, DESY

Talk presented at the XXI International Conference on High Energy Physics, PARIS 1982



## Introduction

This report gives a short résumée of the two sessions on lepton-hadron scattering. Three topics, namely structure functions, hadronic final states and prompt leptons in beam dump experiments, are summarized here, other topics are found in the summaries of L. Sehgal and V. Barger.

## 1. Structure Functions

Deep inelastic lepton scattering off nucleons or nuclear targets has revealed the composite structure of nucleons. The lepton interacts with the quarks inside the nucleon through neutral and charged spacelike currents. All electroweak phenomena are sofar well described by the standard model based on the gauge group U(1) x SU(2). These electroweak currents are therefore ideal tools to investigate the structure of the nucleon. The given gauge structure implies relations between the structure functions observed in charged lepton experiments and in charged and neutral current induced neutrino and antineutrino experiments. The major interest in measuring structure functions is the understanding of their scaling violation. Rather good and consistant data exist from various experiments on isoscalar targets. Least known is the longitudinal structure function related to the exchange of helicity 0 gauge bosons. Another class of experiments deals with lepton scattering off simple targets like hydrogen and deuterium. Although such experiments are based on smaller statistics they are of importance in disentangling the flavour composition of the quarks in the nucleon. Furthermore, in comparing measurements on deuterium with measurements on complex (almost isoscalar) targets nuclear effects may be tested.

This topic can be kept short, since F. Eisele is dealing extensively with structure functions in his plenary talk. Table 1 summarizes the contributions to this Conference.

(a) Gross-Llewellyn-Smith sumrule

This sumrule, $\int_0^1 F_3(x)dx = \#q - \#\overline{q} = 3 \ (Q^2 \rightarrow \infty)$, originally derived from current algebra measures the number of valence quarks in the nucleon, which equals 3 in the quark model. Fig. 1 shows the data of two experiments [3,4]. The errors are statistical. The sumrule is satisfied even at low $Q^2$, provided the contribution of elastic events is included. No or little variation with $Q^2$ is observed. It should, however, be noted that the integral gets important contributions at small x. For fixed $Q^2$ and given neutrino energy spectrum there is a smallest value of x. The small x region is therefore parametrized as $xF_3(x) = Ax^a$ with a = 0.5.

(b) R

New data were presented by CDHS [8], EMC $\mu H_2$ and $\mu Fe$ [10] and BCDMS [10].
$R = \sigma_L/\sigma_T \approx F_L/F_2$ is related to the longitudinal structure function $F_L \equiv F_2 - 2xF_1$. In the naive quark parton model $F_L = 0$ (Callan-Gross relation). R is important for the extraction of $F_2$. The differential $\mu$ and $\nu + \overline{\nu}$ cross sections are proportional to $1 + (1-y)^2 - y^2R$ and thus rather insensitive to R. The CDHS collaboration has

presented considerably improved values for R at large x (see fig. 2). The idea of the new method consists in exploiting the quantity

$$A \equiv \frac{d^2\sigma^{\bar{\nu}} - (1-y)^2 d^2\sigma^{\nu}}{d^2\sigma^{\nu} - (1-y)^2 d^2\sigma^{\bar{\nu}}} = \frac{(1-y)F_L + (1+(1-y)^2)\frac{1}{2}(2xF_1 - xF_3)}{(1-y)F_L + (1+(1-y)^2)\frac{1}{2}(2xF_1 + xF_3)} \approx$$

$$\approx \frac{\bar{q}(x)}{q(x)} + \frac{1-y}{1+(1-y)^2} \quad \frac{F_L}{xq(x)}$$

At large x the quantity A is known experimentally to be nearly zero, thus a tight upper limit can be obtained for R. Averaging over $0.4 < x < 0.7$ gives $\langle R \rangle \leqq 0.006 \pm 0.012 \pm 0.025$. In the region $x < 0.4$ R is still badly measured.

(c) $F_2$, $xF_3$

New results from various experiments (see table 1) were presented. The high statistics experiments with final results agree in shape with each other at the 10-15% level. However, the preliminary data presented by the CCFRR collaboration [4] disagree systematically when compared, for instance, with the data of the CDHS collaboration [5]. Already the quantities $\frac{1}{E}(\sigma^{\nu} + \sigma^{\bar{\nu}})$ measured in the CCFRR experiment show a substantial energy dependence, unless the deviation from constant behaviour be ascribed to normalization differences. It should be noted that this experiment consists of a combination of 5 independent beam settings.
The new, preliminary data of the BCDMS collaboration [10] will be discussed in context with other data by F. Eisele.
The EMC collaboration [10] has extracted the structure function $F_2$ both from their iron and deuterium data. The ratio is plotted in fig. 3 versus the scaling variable x and is not constant, as naively expected, but decreases systematically with increasing x by about 30%. No explanation has as yet been put forward. This effect underlines the importance of lepton scattering experiments using simple targets like hydrogen and deuterium.

(d) NC x-distribution

The CHARM collaboration [9] has contributed a new piece of information in measuring the x distributions in $\nu$ and $\bar{\nu}$ neutral current reactions. Under simplifying assumptions one obtains:

$$F_{\pm}^{NC} \equiv \frac{1}{\sigma_o} \frac{d\sigma^{NC}}{dx} = (\tfrac{4}{3})(u_L^2 + d_L^2 + u_R^2 + d_R^2) F_2^{NC} \pm (\tfrac{2}{3})(u_L^2 + d_L^2 - u_R^2 - d_R^2) xF_3^{NC}$$

where $u_{R,L}$, $d_{R,L}$ are the neutral current couplings and $\pm$ referring to $\nu$ resp. $\bar{\nu}$.
The nucleon structure functions in neutral current interactions (see fig. 4) show

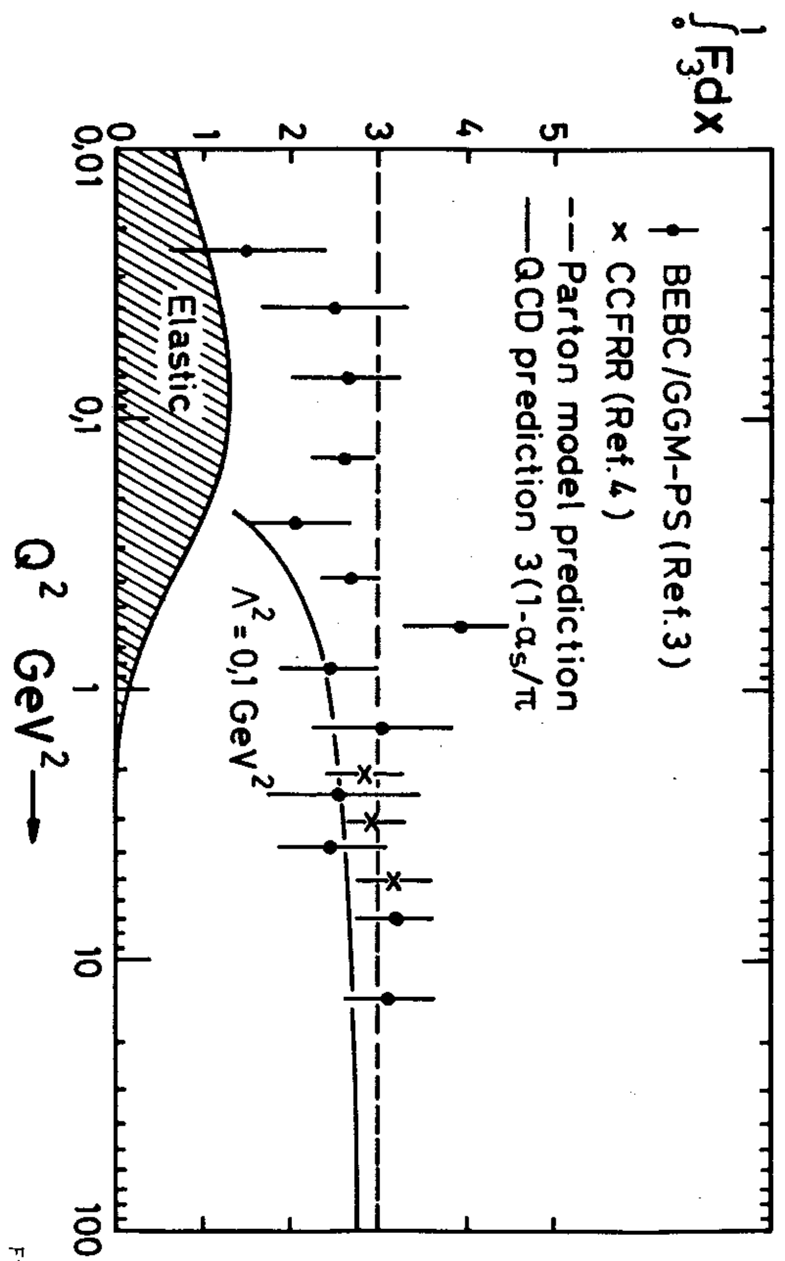


Fig. 1

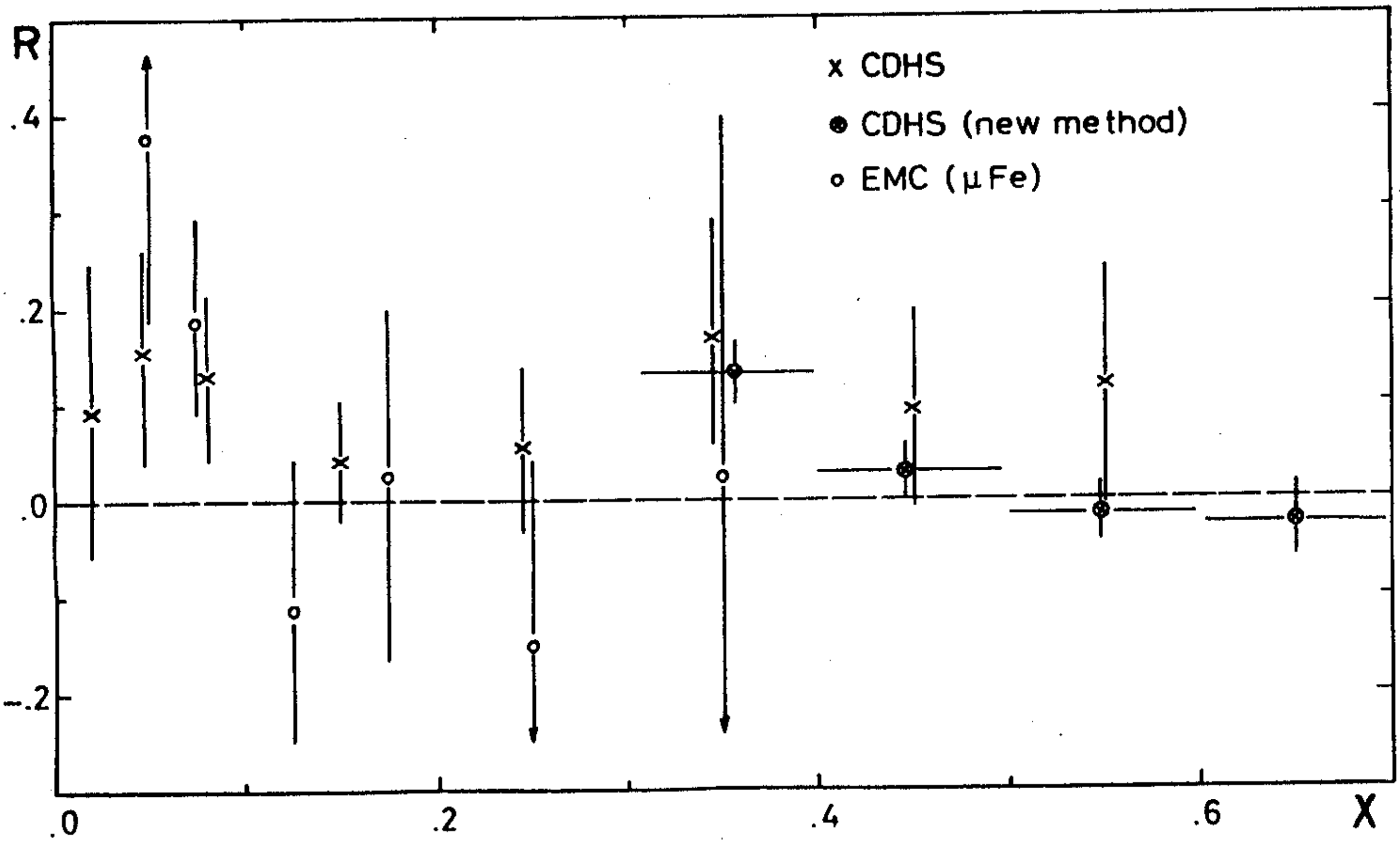

R
.4
.2
.0
-.2
x CDHS
⊗ CDHS (new method)
o EMC (μFe)
.0
.2
.4
.6
X


Fig. 2

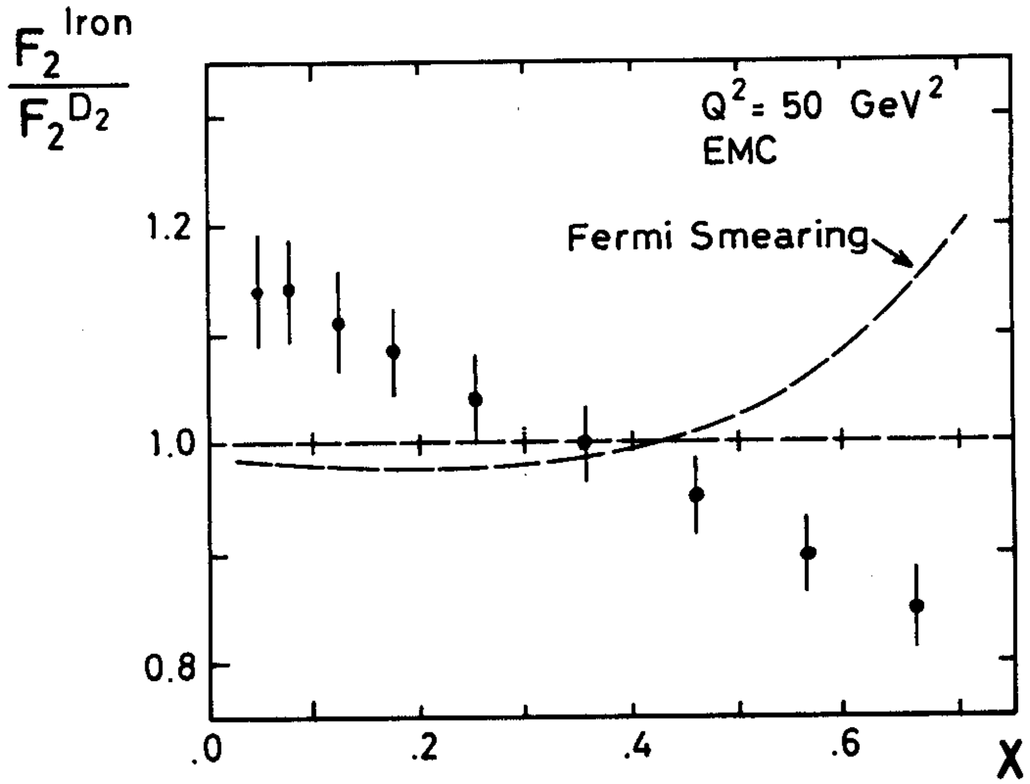

$\frac{F_2^{Iron}}{F_2^{D_2}}$
Q² = 50 GeV²
EMC
Fermi Smearing
1.2
1.0
0.8
.0
.2
.4
.6
X


Fig. 3

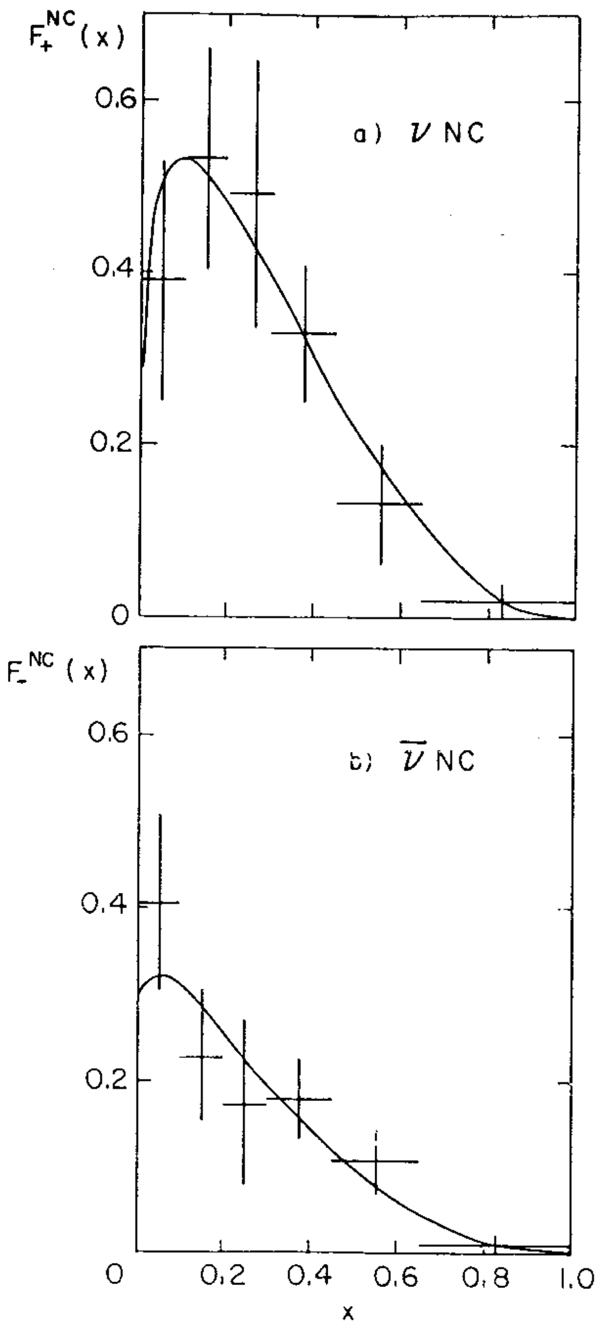


Fig. 4

no significant difference to those measured in charged current interactions as expected by the quark model and the standard model of electroweak interactions.

(e) Parton structure functions

The sea quark distribution $x\bar{q}(x,Q^2) = x(\bar{u} + \bar{d} + 2\bar{s})$ is well measured [5]. With their $\bar{\nu}$ induced opposite sign dimuon sample the CDHS collaboration has deduced the structure function of the strange sea [7]. It agrees in shape with the measured antiquark distribution $\bar{q}$. Using further assumptions they get

$$\frac{2s}{\bar{u} + \bar{d}} = 0.52 \pm 0.09$$

which suggests a nonsymmetric sea. However, $\bar{d}/\bar{u}$ is compatible with 1 within 30% [8].

Three collaborations have presented results on the ratio of the d and u structure functions [1,8,10]. The data agree with each other (fig. 5) for $x > 0.3$. The CDHS group deduced the valence distributions. No data exist beyond $x = 0.8$, where theoretical models give different predictions.

The charmed sea is still rather badly known.

The gluon distribution function is derived by the CDHS collaboration [6] from the $Q^2$ evolution of $F_2$ and $x\bar{q}$.

| Experiment | Quantity | Speaker | Contr. Paper | Reference |
|---|---|---|---|---|
| BEBC | | | | |
| ABCMO $\nu,\bar{\nu}$ $H_2$ | d/u | Schmid | # 596 | 1 |
| ABCDLOS $\nu,\bar{\nu}$ Ne | $F_2$, $xF_3$ | | | 2 |
| BEBC-GGM | $\int F_3$ | | | 3 |
| CCFRR $\nu,\bar{\nu}$ Fe | $F_2$, $xF_3$, $\int F_3$ | Shaevitz | | 4 |
| CDHS $\nu,\bar{\nu}$ Fe | $F_2$, $xF_3$, $\bar{q}$ | | # 708 | 5 |
| | $xG(x)$ | | # 706 | 6 |
| | $xs(x)$ | | # 318 | 7 |
| | R | Merlo | | 8 |
| CDHS $\nu,\bar{\nu}$ $H_2$ | $d_v/u_v$, $\bar{d}/\bar{u}$ | Merlo | | 8 |
| CHARM $\nu,\bar{\nu}$ | NC x-distr. | | # 590 | 9 |
| BCDMS $\mu$C | $F_2$, R | Edwards | | 10 |
| EMC $\mu$Fe, $H_2$, $D_2$ | $F_2^{IRON}/F_2^{D2}$, R | Edwards | | 10 |
| | $F_2^p$, $F_2^n$, d/u | Edwards | | 10 |
| | $F_2$ | | # 749 | 11 |

Table 1: Contributions to this Conference

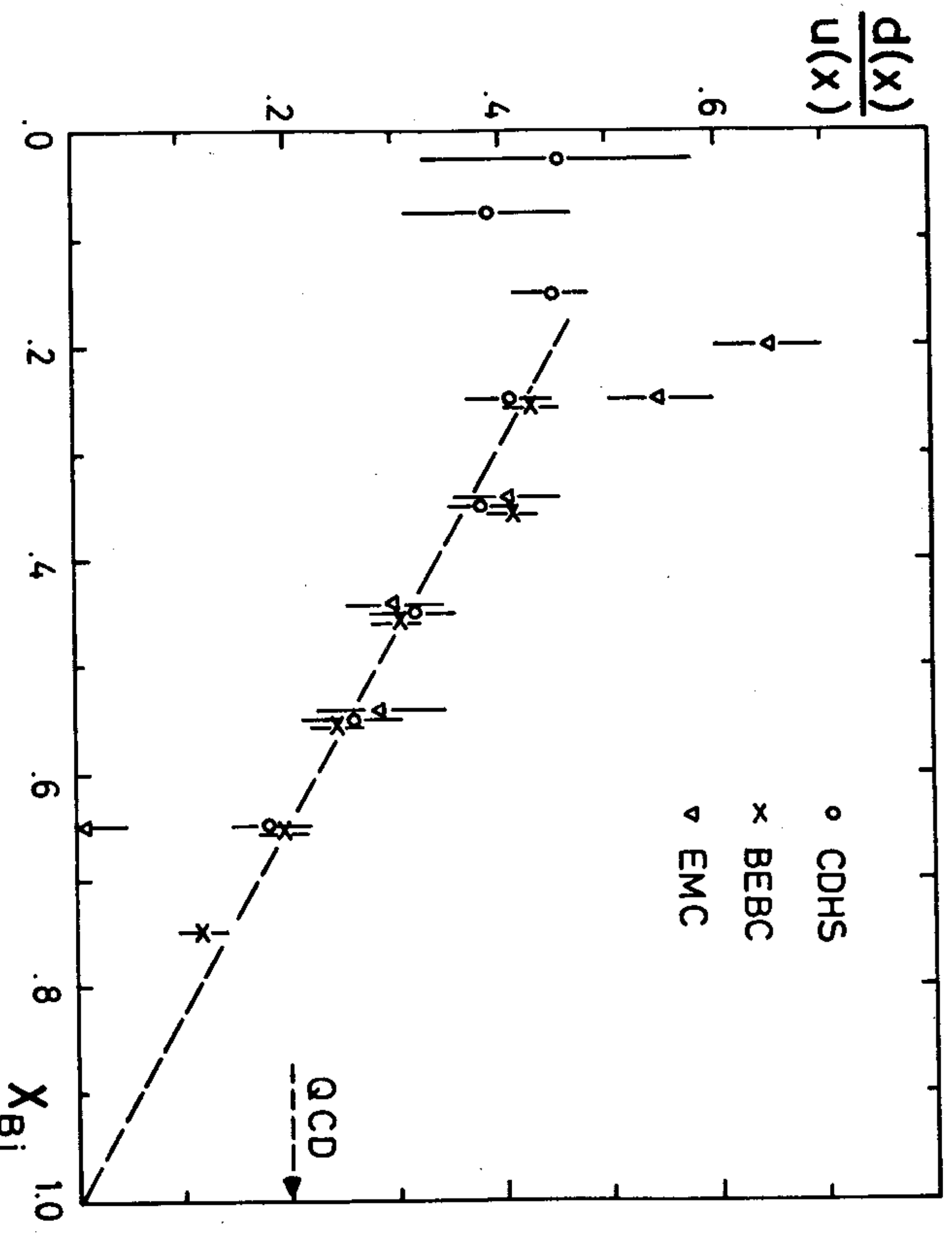


Fig. 5

## 2. Results on Hadronic Final States

New results on final states in lepton-hadron scattering experiments are summarized in table 2. Some contributions are already in their final form and published. They will not be commented here.

(a) Multiplicity

Four bubble chamber experiments presented data on charged hadron multiplicities. The following table shows that the sizes of the ν and $\bar{\nu}$ event samples are quite substantial.

| Experiment | SKAT | 15' | BEBC | BEBC |
|---|---|---|---|---|
| Liquid | Freon | $D_2$ | $H_2$-TST | $H_2$ |
| # ν | 4940 | 11467 | 1000 | 11400 |
| # $\bar{\nu}$ | 1493 | | 400 | 4120 |
| Contr. Paper | 348 | 456 | 612 | 712 |

Two groups emphasize the importance of correct mass assignment. The BEBC-TST group has developped a method to identify protons in the final state [15]. The ABCMO collaboration [13] (BEBC-WA21) performed a thorough study using the LUND Monte Carlo [20] and found that about 17% of the positive and about 8% of the negative hadrons migrate from the backward to the forward hemisphere in the hadrons' centre of mass system, on account of systematics, whereas only 2% from forward to backward.
Due to the poor detection of neutrals in bubble chambers filled with light liquids the effect of the neutrino energy estimation must be carefully taken into account. As a consequence the multiplicity distributions of forward and backward particles are now modified compared to the results presented at the Bonn conference [36]. Fig. 6 shows their corrected multiplicity distributions [13] with the observation that for νp $\langle n_F^+ \rangle$ less than $\langle n_B^+ \rangle$ and for $\bar{\nu}$p $\langle n_F^+ \rangle \approx \langle n_B^+ \rangle$. The ν-data of the BEBC-TST collaboration confirm this behaviour.
The experiment in the SKAT bubble chamber [24] provides data at smaller centre of mass energies ranging from threshold until $W^2 \approx 15$ GeV$^2$. The dispersion $D_-$ depends linearly upon $\langle n_- \rangle$ except for very low average multiplicities of negative hadrons.
In the experiment using the FNAL 15' bubble chamber [18] filled with deuterium multiplicity distributions on protons and neutrons are obtained (fig. 7).

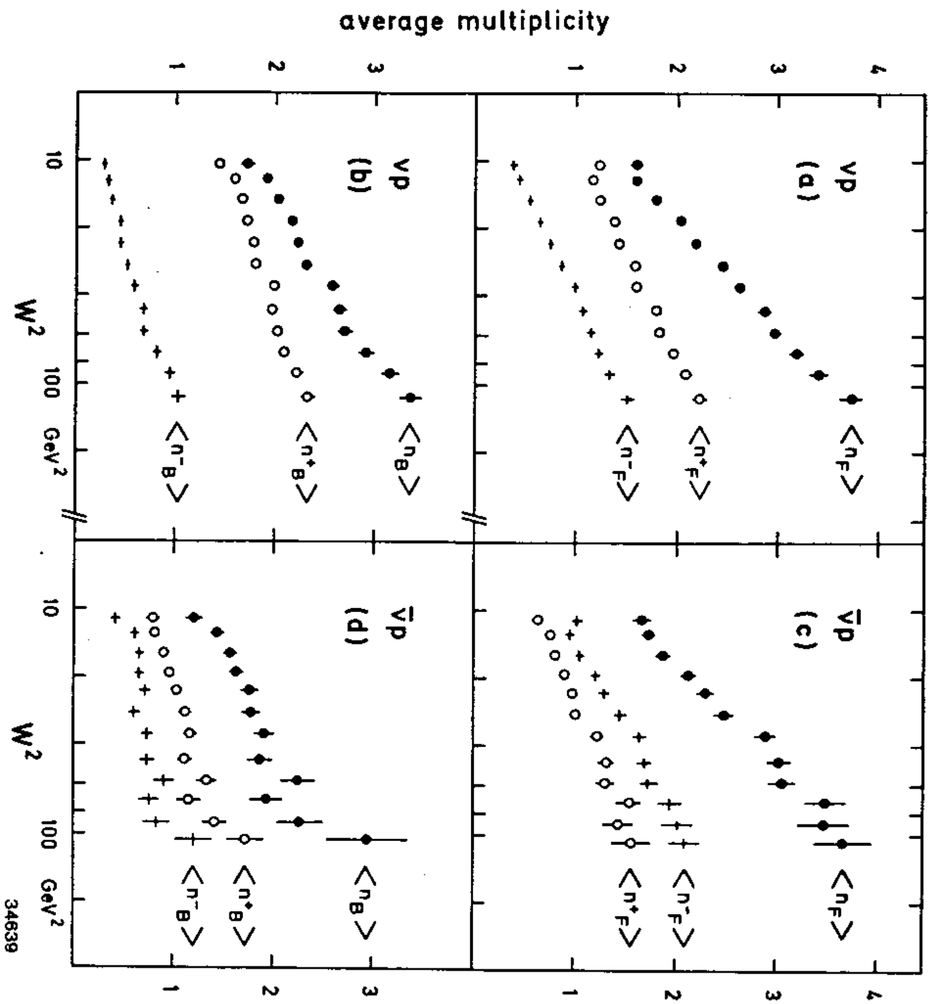


Fig. 6

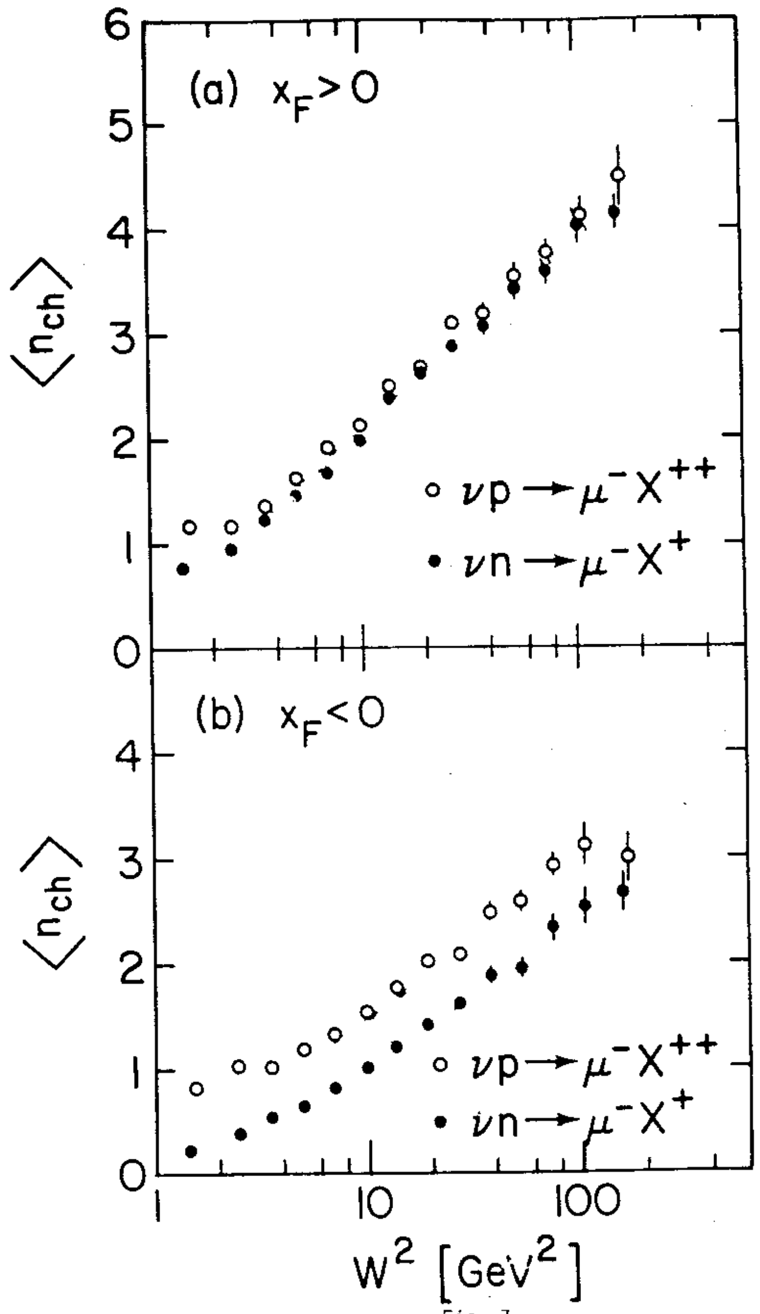

Fig. 7



Many features of the data can be qualitatively understood in terms of q- and qq-fragmentation [37]. For instance, the multiplicity of forward hadrons (u-quark fragments) should be the same in $\nu p$ and $\nu n$, whereas the backward multiplicity in $\nu p$ (due to uu-fragments) should be bigger than in $\nu n$ (due to ud-fragments). This is born out in fig. 7. The relation between dispersion $D_-$ and $<n_->$ appears to be the same for $\nu p$ and $\nu n$ [18].

(b) Charm Fragmentation

The CDHS [7] and the EMC [31] collaborations have presented measurements of the charm fragmentation function using their multi-muon data. The momentum spectrum of $\mu^+$ in $\nu_\mu$-induced charged current interactions contains information on charm fragmentation. The basic process is $\nu_\mu(d,s) \to \mu^- c$ and $c \to \mu^+ \nu_\mu(s,d)$. Fig. 8 shows fits to the measured $\mu^+$ distribution and the extracted charm distribution. The average fractional momentum of the charmed hadron is $<z> = 0.68 \pm 0.08$ including uncertainties due to branching ratios of D-mesons, $\pi/K$ background and charmed quark mass.

The EMC collaboration finds also that the charm fragmentation function is hard as opposed to the soft u,d,s quark fragmentation functions. Their data on dimuons and trimuons are well described by the photon gluon fusion model [30,31]. Fitting the function $D_c(z) \sim \exp(az)$ they obtain $a = 1.6 \pm 1.6$, where the error contains systematic uncertainties of the model parameters, in particular the shape of the gluon distribution function. In the fig. 9 two fragmentation schemes are shown.

(c) Inclusive Particle Production

The LUND model [20] describes fairly well deep inelastic lepton hadron scattering. It treats both quark and diquark fragmentation and accounts, therefore, for meson and baryon production. The ABBPPST collaboration [16] (BEBC-WA 25) with their $\nu$ and $\bar{\nu}$ interactions on deuterium has a unique testing ground for the flavour dependence of quark and diquark fragmentation. Rather than comparing the corrected, unfolded data with the model predictions, they have built into the model all known experimental uncertainties, like neutrino energy correction, mass assignments, resolution, kinematical cuts etc. and compare directly with the uncorrected data. Based on about 6500 $\nu p + \nu n$ and 3800 $\bar{\nu} p + \bar{\nu} n$ after cuts ($W^2 > 5$ GeV$^2$, $Q^2 > 1$ GeV$^2$) the prediction of the LUND model for the Feynman $x_F$-distributions agrees well with the data both for $x_F > 0$ (current fragmentation region) and $x_F < 0$ (target fragmentation region). A detailed study of strange particle production has been carried out. The observed rates and $x_F$-distributions for $K^0$ and $\Lambda$ production are well reproduced provided the fragmentation parameter describing the fraction of $s\bar{s}$ pairs compared to any $q\bar{q}$ pairs in the cascade is assumed to be 0.15. Features like the narrow x-distribution of $\Lambda$'s produced in $\bar{\nu} n \to \mu^+ \Lambda$ + anything, ascribed to interactions with the

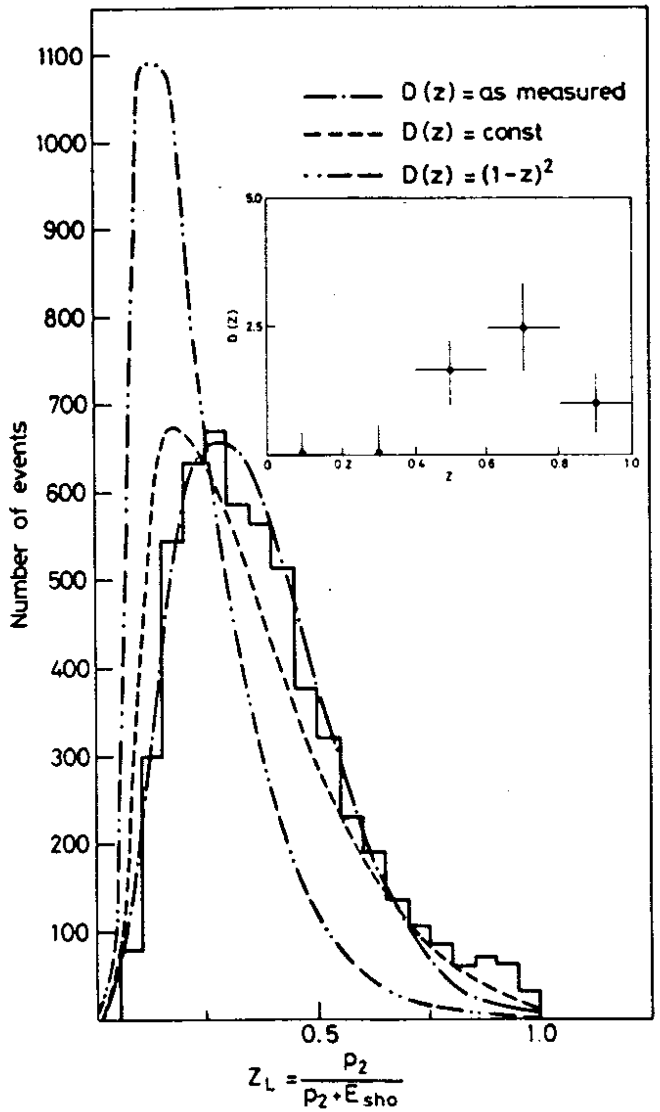
D (z) = as measured
D (z) = const
D (z) = (1 - z)²
Number of events
Z_L = p₂ / (p₂ + E_sho)
D (z)
z

Fig. 8

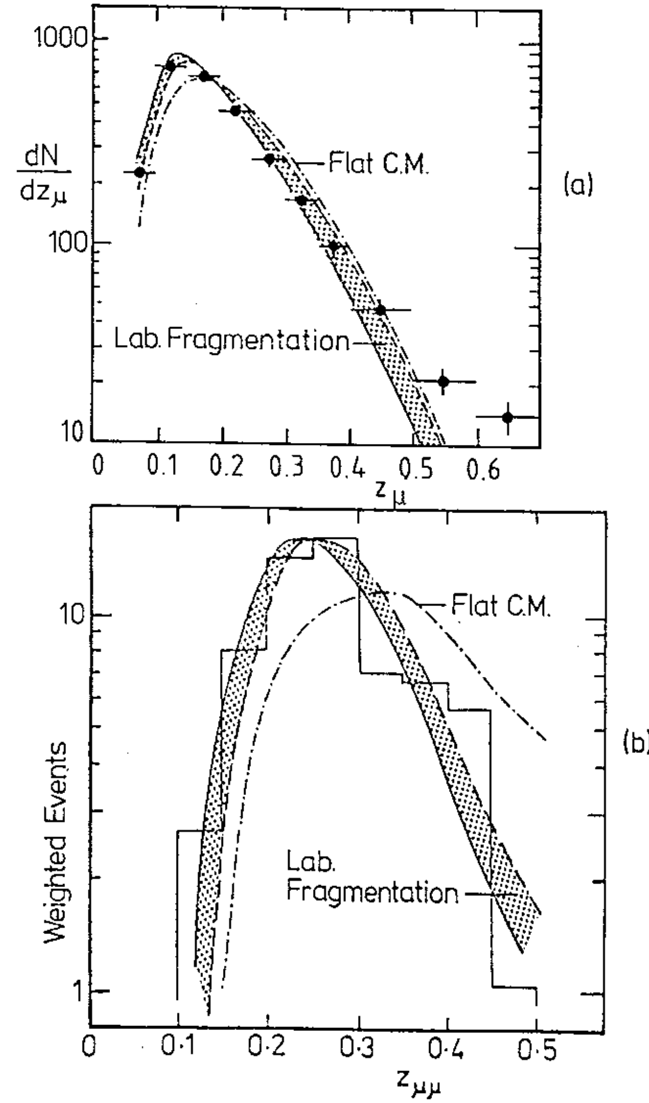
dN/dz_μ
Flat C.M.
Lab. Fragmentation
z_μ
(a)
Weighted Events
Flat C.M.
Lab.
Fragmentation
z_μμ
(b)

Fig. 9

strange sea in the nucleon, are well reproduced. Incidentally, given this interpretation about 45% of the $\Lambda$ in $\bar{\nu}n \to \mu^+\Lambda + x$ are predicted to be produced in association with a charmed particle. Also the production of strange resonances ($K^{*\pm}$ (892), $\Sigma$ (1385)) has been investigated and found to play an important rôle. Fig. 10 shows the $x_F$-distribution of $K^{*+}$ and $K^{*-}$ produced in $\nu$ charged current interactions. Again, good agreement in rate and shape with the LUND model is found. The data on strange baryon production imply that the diquark does not always fragment as one unit, but breaks up with a probability of about 50%.
The EMC collaboration [32] deduced the ratio

$$\rho^0/\pi^0 = 1.0 \pm 0.3 \pm 0.4$$

which implies a production rate of vector to pseudoscalar particles in the Field-Feynman jet model compatible with 1. The EMC-NA9 collaboration has shown first results based on their vertex detector [32]. With this detector it will be possible to investigate also the target fragmentation region.
$\Lambda_c^+$ production has been investigated in a neutrino deuterium experiment by the IIMST collaboration [19] yielding

$$\frac{\sigma(\nu D \to \mu^-\Lambda_c^+ x)\ B(\Lambda_c^+ \to \Lambda x')}{\sigma_{cc}} = (2.1 \pm 0.7 \pm 0.4)\%$$

More results on proton and antiproton production in the current region have been presented by the EMC collaboration [32]. Fig. 11 shows a strong increase of the relative baryon rates with increasing transverse momentum with respect to the jet axis.
Neutral current induced $\psi$ production has been observed by the CDHS collaboration [22].

Charged and strange particle production has also been studied in low energy $\nu$ and $\bar{\nu}$ interactions observed in the bubble chamber SKAT filled with freon [23,24]. At these energies events are not yet jetlike.

(d) cos$\phi$ distribution

Two collaborations have investigated the azimuthal dependence of charged hadrons in the current fragmentation region with respect to the lepton scattering and the hadron production plane. First order QCD expectation is $\langle\cos\phi\rangle \approx -0.1$, but also on the basis of the quark parton model with primordial $k_T$ an effect proportional to $-k_T/Q$ is predicted.
The BEBC-WA59 collaboration [17] observe in their $\bar{\nu}$-data the following averages of cos$\phi$ for $\pi^+$ and $\pi^-$:

| $\langle\cos\phi\rangle$ | $\pi^+$ | $\pi^-$ | $\pi^+$-$\pi^-$ |
|---|---|---|---|
| Data | 1.10 ± 0.45 | -1.52 ± 0.45 | -2.62 ± 0.60 |
| MC | 0.0 ± 0.7 | 1.29 ± 0.45 | 1.30 ± 0.8 |

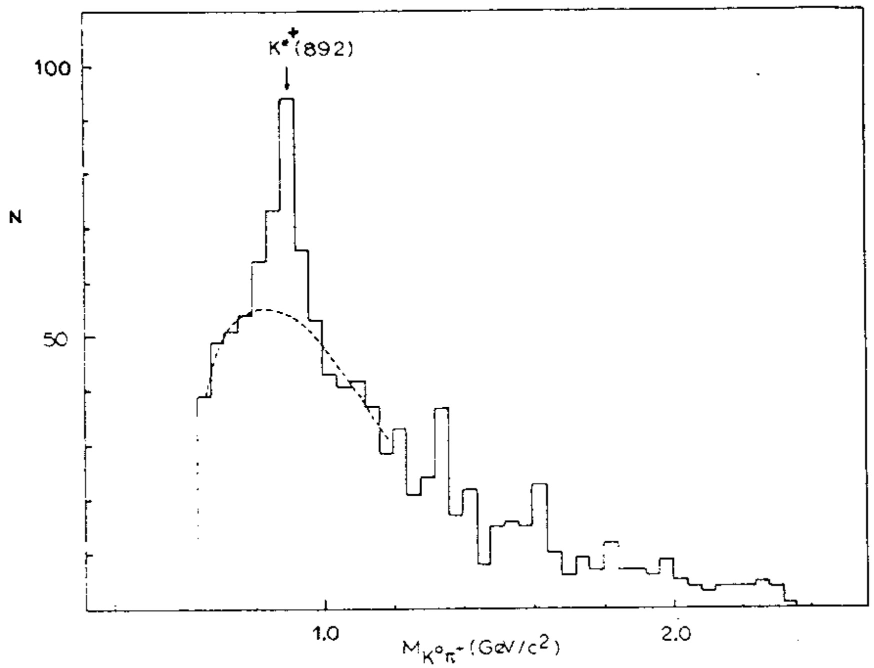


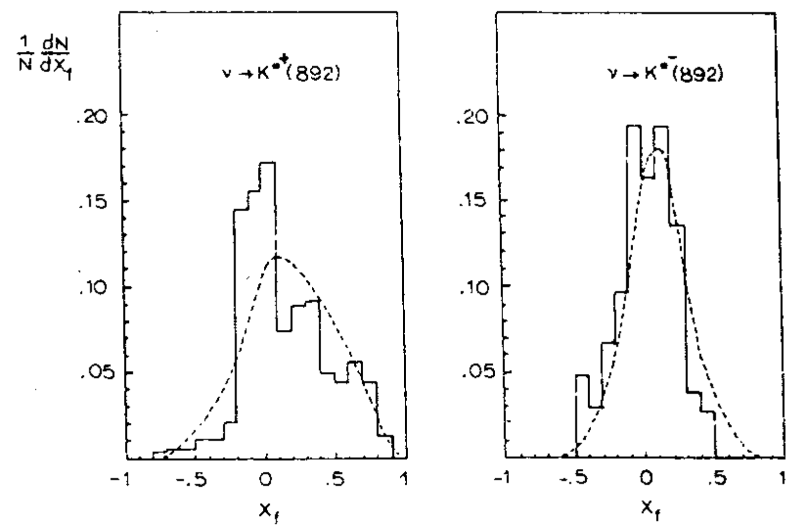


Fig. 10

Systematic effects have been determined by a Monte Carlo calculation assuming a flat $\phi$-dependence. The data show that $<\cos\phi>$ is significantly negative. Also $\pi^0$'s have been investigated. The invariant mass distribution of $\gamma$ and $\mu$ show an enhancement at $M^2 < 0.014$ ascribed to muon bremsstrahlung. Inner muon bremsstrahlung is studied in a contribution to this conference [21] in the FNAL experiment E 546 ($\nu$ Ne/$H_2$ 15') and found in agreement with the QED prediction.
The EMC collaboration [26] observes clearly a negative $<\cos\phi>$. Fig. 12c shows that the effect increases with increasing z. Furthermore, $<\cos2\phi>$ is very small and positive.

(e) Transverse Momentum Flow

The EMC collaboration [27] has found that the transverse momentum of fast forward hadrons is partially compensated by other forward hadrons, as shown in fig. 13.
The LUND model accounts for this behaviour by allowing for soft gluon emission [33]. Then, a value of $<k_T^2>$ as low as 0.2 GeV/$c^2$ is sufficient to provide a good fit to the distribution.

(f) A-Dependence

A comparison of charged hadron production in muon nucleus scattering for various nuclei using the EMC apparatus [29] shows no substantial A-dependence (fig. 12a,b).

(g) $Q^2$-Evolution

The $Q^2$ dependence of charged hadron fragmentation functions have been studied by EMC [28] and BEBC-WA25 [16] and appears to be small.

3. Beam Dump Experiments

There were two presentations on prompt lepton production. The Neutrino beam dump experiment E-613 of the MWOWF collaboration [34] with a full and a 1/3 density tungsten dump yielded 830 single muon and 752 muonless events. The prompt signal is obtained by extrapolation to infinite density. If central production of $D\bar{D}$ gives rise to the observed prompt neutrino interactions the $D\bar{D}$ production cross section parametrized as

$$E \frac{d\sigma}{d\vec{p}} \sim (1-|x|)^n e^{-ap_T}$$

results in (16 ± 3 ± 3) μb for n = 3 and a = 2. There is no evidence for an important $\Lambda_c\bar{D}$ diffractive charm production. The rate of $\#\nu_e/\#\nu_\mu$ is found consistant with 1 provided $E_\nu > 30$ GeV.
Further results dealing with supersymmetry limits [34] are discussed in the talk of L. Sehgal.

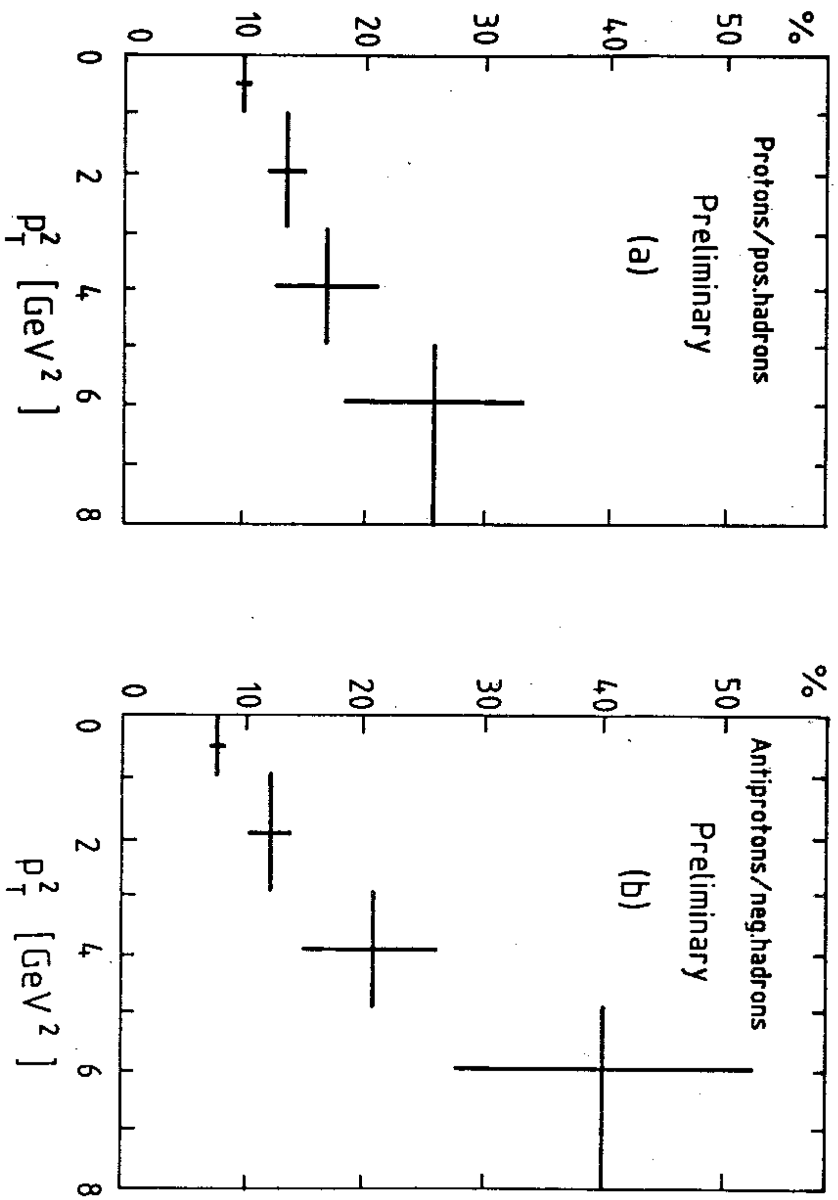


Fig. 11

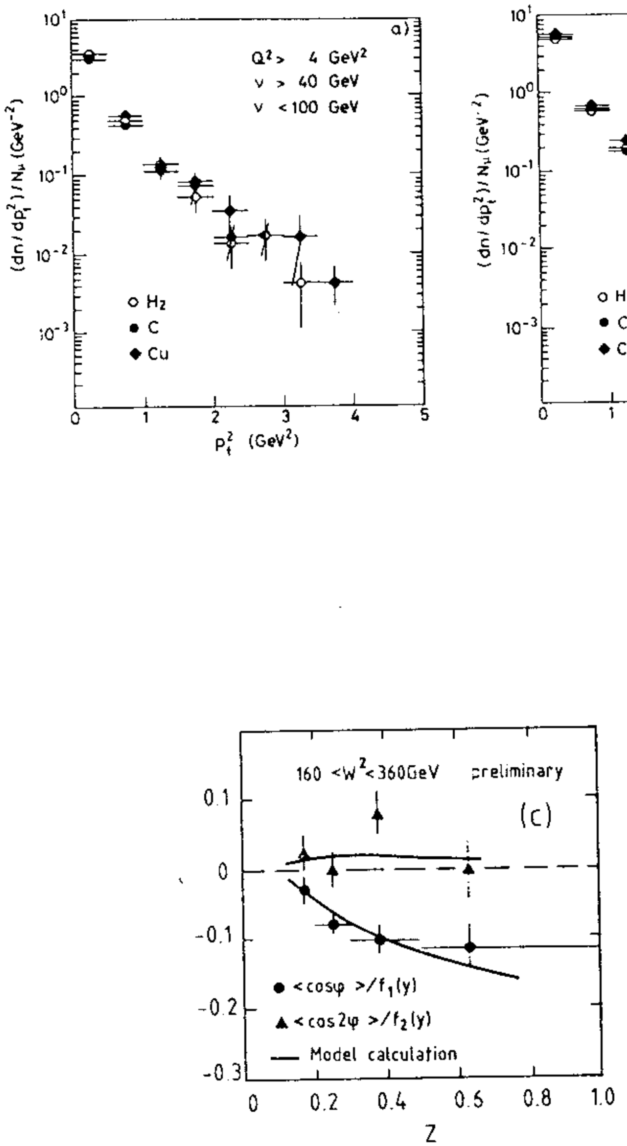
a)
$Q^2 > 4$ GeV$^2$
$\nu > 40$ GeV
$\nu < 100$ GeV
$(dn/dp_t^2)/N_\mu$ (GeV$^{-2}$)
$p_t^2$ (GeV$^2$)
H$_2$
C
Cu
b)
$Q^2 > 4$ GeV$^2$
$\nu > 100$ GeV
$\nu < 160$ GeV
$(dn/dp_t^2)/N_\mu$ (GeV$^{-2}$)
$p_t^2$ (GeV$^2$)
H$_2$
C
Cu
$160 < W^2 < 360$GeV
preliminary
(c)
$< \cos\varphi > / f_1(y)$
$< \cos 2\varphi > / f_2(y)$
Model calculation
Z

Fig. 12

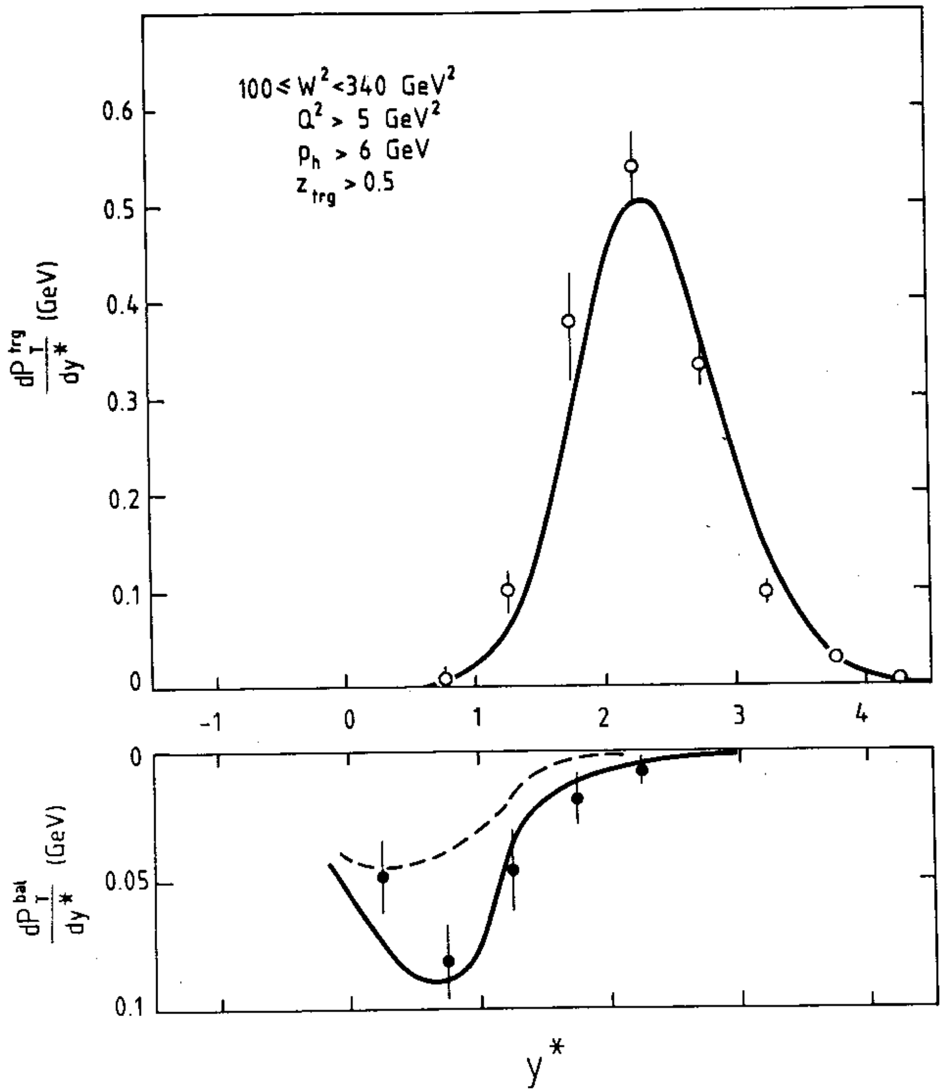
$100 \leq W^2 < 340$ GeV$^2$
$Q^2 > 5$ GeV$^2$
$p_h > 6$ GeV
$z_{trg} > 0.5$
$\frac{dP_T^{trg}}{dy^*}$ (GeV)
$\frac{dP_T^{bal}}{dy^*}$ (GeV)
$y^*$

Fig. 13

Forward production of charmed particle states and prompt muons have been studied in 350 GeV p iron and 278 GeV $\pi^-$ iron beam dump experiment E - 595 [35]. The prompt muon rates were found to be

$$\frac{\#\mu^-}{\#\mu^+} = 1.10 \pm 0.21 \text{ in p Fe} \quad \text{and} \quad \frac{\#\mu^-}{\#\mu^+} = 2.23 \pm 0.29 \text{ in } \pi^- \text{ Fe}$$

for $E_\mu > 20$ GeV. The observed momentum distributions are fit, as above, to $(1-x)^n$ resulting in $n = 6 \pm 0.8$ for $\mu^\pm$ in p Fe, but $n = 3.4 \pm 1.0$ resp. $1.3 \pm 0.8$ for $\mu^+$ resp. $\mu^-$ in $\pi^-$ Fe. From the data with $p_\mu > 50$ GeV it can be concluded that the intrinsic charm component in the proton and pion wavefunctions is less than $2.10^{-4}$.

Table 2

| Experiment | Quantity | Speaker | Contr.Paper | Ref. |
|---|---|---|---|---|
| BEBC WA21 | multiplicity | Schmid | # 712 | 13 |
| | charge properties | | # 711 | 14 |
| WA24 | | | # 612 | 15 |
| WA25 | fragmentation | Vignaud | # 543 | 16 |
| WA59 | cos $\phi$ | | # 737 | 17 |
| 15' FNAL IMSTT $\nu D_2$ | multiplicity | Snow | # 456 | 18 |
| | $\Lambda_c$ | Snow | # 756 | 19 |
| IIF $\bar{\nu}$ Ne | $\rho^-$ exclusive | Sehgal | # 303 | |
| | $\mu$ bremsstrahlung | | | 21 |
| CDHS | $\psi$ NC production | | # 704 | 22 |
| | c-fragmentation | | # 318 | 7 |
| SKAT | $K^0$, $\Lambda$ | | # 504 | 23 |
| | $h^\pm$ production | | # 347, # 348 | 24 |
| GGM | | | # 747 | 25 |
| EMC - NA2 | cos $\phi$, $p_T$ | Becks | # 750, # 795 | 26,27 |
| | $Q^2$ evolution | | # 748 | 28 |
| | nuclear targets | | # 751 | 29 |
| | heavy quarkonium | | # 752 | 30 |
| | open charm | | # 773 | 31 |
| | $\rho/\pi$, p, $\bar{p}$ | Becks | | 32 |
| EMC - NA9 | $p_T^2$, y | Becks | | 32 |



Acknowledgements

I would like to thank Drs. J.J. Aubert and R. Petronzio for the kind invitation and their help during the preparation of the talk. I appreciated discussions with Prof. Eisele, Prof. Snow, Drs. K. Becks, J. Gayler, J.P. Merlo, P. Schmid, W. Scott and A. Vayaki. Thanks to Mrs. S. Platz for the careful typing of the manuscript.

Figure Captions

Fig. 1 The Gross-Llewellyn-Smith sumrule as a function of $Q^2$.

Fig. 2 Measurements of $R = F_L/2xF_1$ averaged over the hadron energy as a function of the Bjorken variable x. The data from CDHS with the new method are upper limits.

Fig. 3 Ratio of the function $F_2$ measured on iron and deuterium vs x. The dashed line represents the effect due to Fermi motion. The systematic error (not included) amounts to about 0.1.

Fig. 4 Neutral current x-distributions for $\nu$ and $\bar{\nu}$ interactions.

Fig. 5 Ratio of quark structure functions d(x)/u(x) vs x.

Fig. 6 Average charged multiplicities in forward and backward hemispheres vs $W^2$. Data from ref. 1.

Fig. 7 Average charged multiplicities in forward and backward hemispheres vs $W^2$. Data from ref. 18.

Fig. 8 Distribution of neutrino dimuon events as a function of $z_L$ determined by the momentum of the decay muon and the hadron shower energy. The curves are comparisons with Monte Carlo predictions. The inlet shows the fitted charm fragmentation function.

Fig. 9 Energy distributions of decay muons from charmed meson decays
a) $Z_\mu = E_\mu/E_{had}$ for dimuon events
b) $Z_{\mu\mu} = (E_{\mu 1} + E_{\mu 2}) / E_{had}$ for trimuon events.

Fig. 10 Invariant mass distribution of $K^0$ and $\pi^+$ with $(K^*)^+$ peak and x-Feynman distributions of $(K^*)^\pm$ observed in $\nu$-induced interactions. Data from ref. 16.

Fig. 11 Relative proton and antiproton production observed by EMC (ref. 32).

Fig. 12 Data from EMC
a,b) hadron production off 3 different nuclei versus $p_T^2$ (ref. 25).
c) Moments of the azimuthal distribution of charged hadrons vs fractional energy (ref. 26).

Fig. 13 Transverse momentum flow and balancing component vs cms rapidity (ref. 27).

## References

[1] Talk by P. Schmid
Contr. Paper # 596, Direct determination of the quark density ratio d(x)/u(x) in the proton from $\nu p$ and $\bar{\nu}p$ interactions, ABCMO Collaboration (BEBC-WA 21)

[2] P.C. Bosetti et al., PITHA 82-04 (Aachen Preprint 1982)

[3] T. Bolognese et al., CERN-EP/82-78

[4] Talk by M.H. Shaevitz
R.E. Blair et al., Neutrino Charged Current Structure Functions, UR-831 COO-3065-339

[5] H. Abramowicz et al., (CDHS), Z. Phys. C13 (1982) 199, Contr. Paper # 708

[6] H. Abramowicz et al., (CDHS), Z. Phys. C12 (1982) 289, Contr. Paper # 706

[7] H. Abramowicz et al., (CDHS), Experimental Study of opposite sign dimuons produced in $\nu$ and $\bar{\nu}$ interactions, CERN-EP/82-77 and Contr. Paper # 318

[8] Talk by J.P. Merlo

[9] Contr. Paper # 590, J.V. Allaby et al., (CHARM), CERN-EP/82-85
Experimental Study of x-distributions in semileptonic neutral current neutrino reactions

[10] Talk by A. Edwards

[11] Contr. Paper # 749, J.J. Aubert et al., (EMC), CERN-EP/82-48

[12] H. Abramowicz et al., (CDHS), PL 107 B (1981) 141

[13] Talk by P. Schmid
Contr. Paper # 712, Multiplicities of secondary hadrons produced in $\nu p$ and $\bar{\nu}p$ charged current interactions, ABCMO Collaboration (BEBC-WA21)

[14] Contr. Paper # 711, P. Allen et al., Charge Properties of the hadronic system in $\nu p$ and $\bar{\nu}p$ interactions, MPI-PAE/Exp. El. 103

[15] Contr. Paper # 612, Results on the identification of protons produced in $\nu p$ interactions in BEBC equipped with a TST, BBB EP R UCL Collaboration (BEBC-WA24)

[16] Talk by D. Vignaud
Contr. Paper # 543, Fragmentation of the hadronic system in a $\nu$, $\bar{\nu}$ $D_2$ experiment; comparison with the LUND model, ABBPPST Collaboration (BEBC-WA25)

[17] Contr. Paper # 737, A. Vayaki et al., Azimuthal asymmetry of hadrons produced in $\bar{\nu}$-reactions, BBBCD-EP-IC-MORS-UCL Collaboration (BEBC-WA59)

[18] Talk by G.A. Snow
Contr. Paper # 456, D. Zieminska et al., Charged particle multiplicity distributions in $\nu n$ and $\nu p$ charged current interactions, IMSTT Collaboration (FNAL 15' $D_2$)

[19] Contr. Paper # 756, G.A. Snow et al., Charmed baryon production in $\nu D \to \mu^- \Lambda x$ reactions, IMSTT Collaboration (FNAL 15' $D_2$)

[20] T. Sjöstrand, LUTP-80-3 (LUND 1980)



[21] H.C. Ballagh et al., Observation of muon inner bremsstrahlung in deep inelastic neutrino scattering Events, LBL-F-H-W-W Collaboration (E 546 15'), Contr. Paper #

[22] Contr. Paper # 704, H. Abramowicz et al., (CDHS), PL 109B (1982) 115

[23] Contr. Paper # 504, D.S. Baranov et al., Results on neutral strange particle production in charged current $\nu A$ interactions, IHEP-BERLIN Collaboration (SKAT)

[24] Contr. Paper # 347/8, D.S. Baranov et al., Inclusive charged hadron production in $\nu A$ and $\bar{\nu}A$ interactions: part I and part II, IHEP-Berlin Collaboration (SKAT)

[25] Contr. Paper # 747, Multilepton production by neutrinos in Gargamelle at CERN-SPS energies, BCS-Collaboration

[26] Contr. Paper # 750, J.J. Aubert et al. (EMC), measurement of $\phi$ moments in deep inelastic muon proton scattering

[27] Contr. Paper # 795, J. Gayler et al. (EMC), Balance of transverse momentum in $\mu N$ scattering

[28] Contr. Paper # 748, J.J. Aubert et al. (EMC), Measurement of the $Q^2$, x and $W^2$ dependence of single hadron production in deep inelastic muon scattering, CERN-EP/82-47

[29] Contr. Paper # 751, J.J. Aubert et al. (EMC), Preliminary results in hadron production in 200 GeV $\mu$-copper and $\mu$-carbon interactions

[30] Contr. Paper # 752, J.J. Aubert et al. (EMC), Muon production of heavy quarkonium

[31] Contr. Paper # 773, J.H. Aubert et al. (EMC), Production of open charm in 250 GeV $\mu^+$ iron interactions

[32] Talk by K.H. Becks
K.H. Becks, New results on hadronic final states from the EMC Collaboration, WU B 82-13 (Wuppertal preprint); F.W. Brasse, Hadronic final states in high energy muon nucleon scattering, recent results from EMC, DESY 82-47

[33] G. Ingelman et al., LUND preprint LU TP 81-8 (1981)

[34] Talk by B. Roe
Contr. Paper #    , R.C. Ball et al., Prompt production of $\nu$ by 400 GeV protons on tungsten, UM HE 82-15 and UM HE 82-16 and UM HE 82-21

[35] Talk by A. Bodek
A. Bodek et al., A study of the forward production of charm states and prompt muons in 350 GeV p-Fe and 278 GeV $\pi^-$-Fe interactions, UR-827 COO-3065-335 (1982)

[36] P. Allen et al., Nucl. Phys. B181 (1981) 385

[37] D. Haidt, Jets from hadron-, muon- and neutrino-interactions in comparison with jets in $e^+e^-$-annihilation, Proc. 1981 Int. Symposium BONN, p. 558